Dynamics of Circular Cylindrical Shells under Seismic Loads

Francesco Pellicano

Dept. of Mechanical and Civil Engineering Univ. of Modena and Reggio Emilia, V. Vignolese, 905 – 41100 Modena Tel. 059 2056154 Fax 0592056126 email: francesco.pellicano@unimore.it

Keywords: nonlinear vibration**,** shells**.**

SUMMARY. The present paper is focused on the dynamic analysis of circular cylindrical shells under seismic excitation: the excitation direction is the cylinder axis, the shell is clamped at the base and connected to a rigid body on the top, the base provides the seismic excitation which is supposed sinusoidal. The goal is to investigate the shell response when a resonant forcing is applied: the first axisymmetric mode is excited around the resonance at relatively low frequency and low amplitude excitation. A violent resonant phenomenon is experimentally observed as well as an interesting saturation phenomenon close to the previously mentioned resonance. A theoretical model is developed to reproduce the experimental evidence and provide an explanation of the complex dynamics observed experimentally.

1 INTRODUCTION

The continuous growing of the commercial use of Space facilities lead to the development of new and more efficient aerospace vehicles; therefore, new and accurate studies on light-weight, thin-walled structures are needed. A wide part of the technical literature in the past century was focalized on the analysis of thin-walled structures and tried to investigate their behaviour in many different operating conditions, i.e. under static or dynamic loads, either in presence or absence of fluid-structure interaction. Both linear and nonlinear models have been developed to forecast the response of such structures. Many studies were concerned with cylindrical shells that constitute main parts of aircrafts, rockets, missiles and generally aerospace structures.

The literature about vibration of shells is extremely wide and the reader can refer to Refs. [1,2] for a comprehensive review of models and results present in literature.

Trotsenko and Trotsenko [3], studied vibrations of circular cylindrical shells with attached rigid bodies, by means of a mixed expansion based on trigonometric functions and Legendre polynomials; they considered only linear vibrations.

The literature analysis shows that in the past several methods were developed for investigating: *i*) linear vibrations of complex shells; *ii*) nonlinear vibrations of shells having simple shape and boundary conditions. Therefore, a contribution toward the knowledge of new dynamic phenomena on shells is welcome.

In the present paper, experiments are carried out on a circular cylindrical shell, made of a polymeric material (P.E.T.) and clamped at the base by gluing its bottom to a rigid support. The axis of the cylinder is vertical and a rigid disk is connected to the shell top end. In Ref. [4] this problem was fully analyzed from a linear point of view. Here nonlinear phenomena are investigated by exciting the shell using a shaking table and a sine excitation. Shaking the shell from the bottom induces a vertical motion of the top disk and, therefore, axial loads due to inertia forces. Such axial loads generally give rise to axial symmetric deformations; however, in some conditions it is observed that a violent resonant phenomenon takes place, with a strong energy transfer from low to high frequencies and huge amplitude of vibration. Moreover, an interesting

saturation phenomenon is observed.

A mathematical model is developed to explain the phenomenon, such model is a semi-analytical approach based on the nonlinear Sanders-Koiter shell equations discretized by means of a mesh-less method. The agreement with experiments is excellent for which concern the linear dynamics and qualitative in the case on nonlinear vibrations.

2 THEORETICAL MODEL: EQUATIONS OF MOTION

In Figure 1 three displacement fields represent the shell deformation: axial $u(x,\theta,t)$, circumferential $v(x,\theta,t)$ and radial $w(x,\theta,t)$; a cylindrical coordinate system is used.

Geometric imperfections can be considered in the theory by means of an initial radial displacement field $w_0(x,\theta)$; however, in the numerical results, only perfect shells are considered.

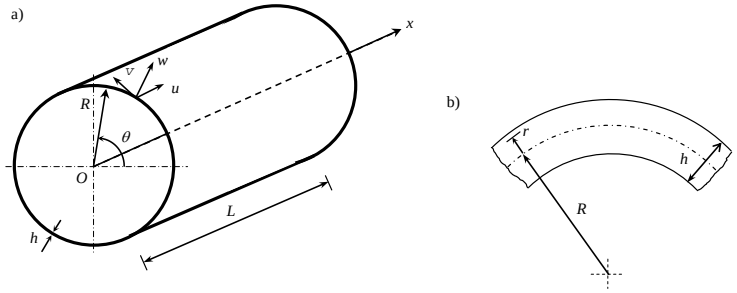

Figure 1. Shell geometry.

Strain Energy

The Sanders-Koiter theory is based on Love's first approximation: (i) $h<<R$; (ii) strains are small; (iii) transverse normal stresses are small; and (iv) the normal to the undeformed middle surface remains straight and normal to the middle surface after deformation, no thickness stretching is present (Kirchhoff-Love kinematic hypothesis) [1,2,5]; (v) rotary inertia and shear deformations are neglected.

Strain components ε_x, ε_θ and $\gamma_{x\theta}$ at an arbitrary point of the shell are ([1]:

$$\varepsilon_x = \varepsilon_{x,0} + r\,k_x \qquad \varepsilon_\theta = \varepsilon_{\theta,0} + r\,k_\theta \qquad \gamma_{x\theta} = \gamma_{x\theta,0} + r\,k_{x\theta} \tag{1}$$

where: $\varepsilon_{x,0}$, $\varepsilon_{\theta,0}$ and $\gamma_{x\theta,0}$ are middle surface strains; k_x, k_θ and $k_{x\theta}$ are curvature and Torsion changes of the middle surface; and r is the distance of the arbitrary point of the shell from the middle surface (see Figure 1(b)). The definition of strain-displacement relationships can be found in [1,2,4].

The elastic strain energy U_S of a circular cylindrical shell, neglecting the radial stress σ_r (Love's first approximation), is given by [5]

$$U_S = \frac{1}{2} LR \int_0^{2\pi} \int_0^1 \int_{-h/2}^{h/2} \left(\sigma_x \varepsilon_x + \sigma_\theta \varepsilon_\theta + \tau_{x\theta} \gamma_{x\theta}\right) \mathrm{d}\eta \,(1 + r/R)\,\mathrm{d}\theta\,\mathrm{d}r\,, \tag{2}$$

In the case of homogeneous and isotropic materials, stresses σ_x, σ_θ and $\tau_{x\theta}$ are related to strains ($\sigma_r = 0$, case of plane stress) [5]

$$\sigma_x = \frac{E}{1-\nu^2}\left(\varepsilon_x + \nu\,\varepsilon_\theta\right),\ \sigma_\theta = \frac{E}{1-\nu^2}\left(\varepsilon_\theta + \nu\,\varepsilon_x\right), \qquad \tau_{x\theta} = \frac{E}{2(1+\nu)}\gamma_{x\theta}, \tag{3}$$

where E is the Young's modulus and ν is the Poisson's ratio.

Using equations (1-3), the following expression of the potential energy is obtained

$$U_S = \frac{1}{2}\frac{E\,h}{1-\nu^2} LR \int_0^{2\pi}\int_0^1 \left(\varepsilon_{x,0}^2 + \varepsilon_{\theta,0}^2 + 2\nu\,\varepsilon_{x,0}\,\varepsilon_{\theta,0} + \frac{1-\nu}{2}\gamma_{x\theta,0}^2 \right) \mathrm{d}\eta\,\mathrm{d}\theta + \frac{1}{2}\frac{E\,h^3}{12\left(1-\nu^2\right)} LR \int_0^{2\pi}\int_0^1 \left(k_x^2 + k_\theta^2 + 2\nu\,k_x\,k_\theta + \frac{1-\nu}{2}k_{x\theta}^2 \right) \mathrm{d}\eta\,\mathrm{d}\theta + O(h^4) \quad (4)$$

where $O(h^4)$ is a higher-order term in h according to the Sanders-Koiter theory.

The first term of the right end side of equation (5) is the membrane energy (also referred to stretching) and the second one is the bending energy.

The kinetic energy T_S of a circular cylindrical shell (rotary inertia is neglected) and the virtual work W done by the external forces are given by

$$T_S = \frac{1}{2}\rho_S\,h\,L\,R \int_0^{2\pi}\int_0^1 \left(\dot{u}^2 + \dot{v}^2 + \dot{w}^2 \right) \mathrm{d}\eta\,\mathrm{d}\theta\,, \qquad W = LR \int_0^{2\pi}\int_0^1 \left(q_x\,u + q_\theta\,v + q_r w \right) \mathrm{d}\eta\,\mathrm{d}\theta \quad (5)$$

where ρ_S is the mass density of the shell, the overdot denotes a time derivative and q_x, q_θ and q_r are the distributed forces per unit area acting in axial, circumferential and radial directions.

In-plane forces and bending moments depend on the shell strain:

$$M_x = \frac{E\,h^3}{12(1-\nu^2)}\left(k_x + \nu\,k_\theta \right), \qquad N_x = \frac{E\,h}{1-\nu^2}\left(\varepsilon_{x,0} + \nu\,\varepsilon_{\theta,0} \right). \quad (6)$$

3 LINEAR VIBRATION: MODAL ANALYSIS.

In order to carry out a linear vibration analysis, in the present section, linear Sanders-Koiter theory is considered, i.e. in equation (5), only quadratic terms are retained.

The best basis for expanding displacement fields is the eigenfunction basis, but only for special boundary conditions such basis can be found analytically; generally, eigenfunctions must be evaluated in approximate way.

In order to attack the general problem of circular cylindrical shell vibration, displacement fields are expanded by means of a double series: the axial symmetry of the geometry and the periodicity of the deformation in the circumferential direction, leads to use harmonic functions; Chebyshev polynomials are considered in the axial direction.

Let us now consider a modal vibration, i.e. a synchronous motion:

$$u(\eta,\theta,t)=U(\eta,\theta)\,f(t) \qquad v(\eta,\theta,t)=V(\eta,\theta)\,f(t) \qquad w(\eta,\theta,t)=W(\eta,\theta)\,f(t) \quad (7)$$

where: $U(\eta,\theta)$, $V(\eta,\theta)$ and $W(\eta,\theta)$ represent the modal shape.

The modal shape is now expanded in a double series, in terms of Chebyshev polynomials $T_m^*(\eta)$ and harmonic functions:

$$U(\eta,\theta) = \sum_{m=0}^{M_U}\sum_{n=0}^{N} \tilde{U}_{m,n} T_m^*(\eta)\cos n\theta\,, \; V(\eta,\theta) = \sum_{m=0}^{M_V}\sum_{n=0}^{N} \tilde{V}_{m,n} T_m^*(\eta)\sin n\theta\,, \; W(\eta,\theta) = \sum_{m=0}^{M_W}\sum_{n=0}^{N} \tilde{W}_{m,n} T_m^*(\eta)\cos n\theta\,, \quad (8)$$

where $T_m^*(\eta) = T_m\left(2\eta - 1\right)$ and $T_m(\cdot)$ is the m-th order Chebyshev polynomials.

Expansions (8) do not satisfy any particular boundary condition.

3.1 *Boundary conditions*

In the present work boundary conditions are considered by applying constraints to the free coefficients of expansions (8). Some of the coefficients $\tilde{U}_{m,n}$, $\tilde{V}_{m,n}$ and $\tilde{W}_{m,n}$ of the equation (8) can be suitably chosen in order to satisfy boundary conditions, see Ref. [4] for analytical details.

In case of shells carrying a top disk both theoretical, experimental and finite elements analyses were carried out in Ref. [4]; in Figure 2 the geometry of the system as well as the dimensions are represented, the scheme corresponds to the experimental setup of Figure 3.

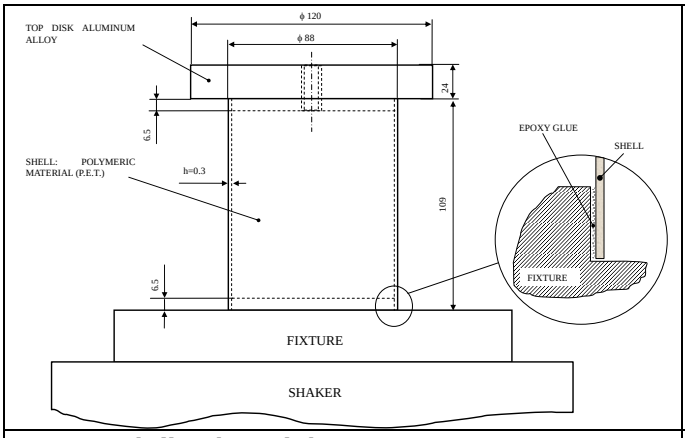

Figure 2. Shell with top disk: representation.

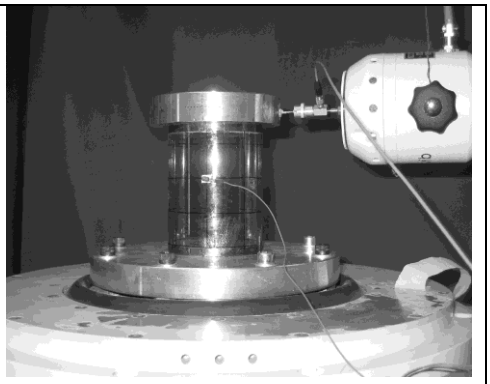

Figure 3. Shell with top disk: experimental setup.

The shell is clamped at the bottom to a rigid support; therefore, for η=0 the boundary conditions are clamped.

In order to impose boundary conditions to the top end of the shell, it is useful to consider the rigid body motion of the disk. Such a body has six degrees of freedom; however, in the present work torsional vibration is not considered; therefore, the number of degrees of freedom is reduced to five.

Three displacements of the disk are considered S_{Dx}, S_{Dy}, S_{Dz} see Ref. [4] and two rotations about horizontal axes α_y and α_z. Such displacements and rotations induce specific displacements on the shell top end.

It is to note that, for n>1 boundary conditions given by the rigid body motion correspond to clamping (see equations 8); moreover, axisymmetric modes (n=0) are influenced by S_{Dx} only.

3.2 *Kinetic energy: disk on the top*

The kinetic energy of the shell is given by equation (5); when a rigid body is connected to one of the shell ends, its kinetic energy must be added to the shell energy.

If one is not interested in torsional vibrations of the shell, the rotation about x axis can be neglected; therefore, the kinetic energy of the disk is given by:

$$T_D = \frac{1}{2} m_D \left(\dot{S}_{Dy} + \dot{\alpha}_z h_G \right)^2 + \frac{1}{2} m_D \left(\dot{S}_{Dz} - \dot{\alpha}_y h_G \right)^2 + \frac{1}{2} J_z \dot{\alpha}_z^2 + \frac{1}{2} J_y \dot{\alpha}_y^2 + \frac{1}{2} m_D \dot{S}_{Dx}^2 \tag{9}$$

where h_G is the position of the centre of mass of the disk in x direction with respect to the centre of the top shell end.

3.3 *Discretization: Lagrange equations*

Equation (7) and expansions (8) are inserted in the expressions of the kinetic and the potential energy (for the linear system); then a set of ordinary differential equations is obtained by using Lagrange equations.

A vector containing all variables is built:

$$\mathbf{q} = \left[..., \tilde{U}_{i,j}, ..., \tilde{V}_{i,j}, ..., \tilde{W}_{i,j}, ..., \tilde{S}_{Dx}, \tilde{S}_{Dy}, \tilde{S}_{Dz}, \tilde{\alpha}_y, \tilde{\alpha}_z \right] f(t) \tag{10}$$

where $S_{Dx} = f(t)\tilde{S}_{Dx}$, $S_{Dy} = f(t)\tilde{S}_{Dy}$, $S_{Dz} = f(t)\tilde{S}_{Dz}$, $\alpha_y = f(t)\tilde{\alpha}_y$, $\alpha_z = f(t)\tilde{\alpha}_z$.

A unique time law $f(t)$ is considered in order to impose a synchronous motion (modal vibration); such assumption will be relaxed in the case of nonlinear vibration.

Lagrange equations for free vibrations are:

$$\frac{d}{dt}\left(\frac{\partial L}{\partial \dot{q}_i}\right)-\frac{\partial L}{\partial q_i}=0 \quad i=1,2,\ldots N_{\max} \tag{11}$$

where N_{max} is the dimension of vector **q**.

Using equation (11) and considering an harmonic motion, $f(t)=e^{j\omega t}$, one obtains:

$$\left(-\omega^2\mathbf{M}+\mathbf{K}\right)\mathbf{q}=\mathbf{0} \tag{12}$$

A modal shape corresponding to the j-th mode is given by equations (8); where: $\tilde{U}_{m,n}$, $\tilde{V}_{m,n}$ and $\tilde{W}_{m,n}$ are substituted with $\tilde{U}^{(j)}_{m,n}$, $\tilde{V}^{(j)}_{m,n}$ and $\tilde{W}^{(j)}_{m,n}$, which are components of the j-th eigenvector of equation (12) and the vector function $\mathbf{U}^{(j)}(x,\theta)=\left[U^{(j)}(x,\theta),V^{(j)}(x,\theta),W^{(j)}(x,\theta)\right]^T$ is the j-th eigenfunction vector of the original problem.

Eigenfunctions are normalized by imposing that the maximum amplitude referred to the dominant direction of a mode shape (radial w, circumferential v or longitudinal u) is equal to 1.

4 NONLINEAR MODEL

In the nonlinear analysis the full expression of potential shell energy (4), containing terms up to fourth order (cubic nonlinearity), is considered. Displacement fields $u(x,\theta,t)$, $v(x,\theta,t)$ and $w(x,\theta,t)$ are expanded by using linear mode shapes obtained in the previous section:

$$u(x,\theta,t)=\sum_{j=1}^{N_{\max}}U^{(j)}(x,\theta)\,f_{u,j}(t) \quad v(x,\theta,t)=\sum_{j=1}^{N_{\max}}V^{(j)}(x,\theta)\,f_{v,j}(t) \quad w(x,\theta,t)=\sum_{j=1}^{N_{\max}}W^{(j)}(x,\theta)\,f_{w,j}(t) \tag{13}$$

Expansions (13) respect boundary conditions, modal shapes $U^{(j)}(x,\theta)$, $V^{(j)}(x,\theta)$, $W^{(j)}(x,\theta)$, are known functions expressed in terms of polynomials and harmonic functions. Similarly to the previous section a reordering of variables is useful: $\mathbf{z}=\left[f_{u,1}, f_{u,2},..., f_{v,1}, f_{v,2},..., f_{w,1}, f_{w,2},...\right]$.

Expansion (13) is put in the strain and kinetic energy and in the virtual work in the case of external excitation. Lagrange equations now read:

$$\frac{d}{dt}\left(\frac{\partial L}{\partial \dot{z}_i}\right)-\frac{\partial L}{\partial z_i}=Z_i=\frac{\partial W}{\partial z_i} \quad i=1,2,\ldots N_{\mathrm{z,max}} \tag{14}$$

Where W is the virtual work of the external excitation that is in the present problem due to the seismic base motion. The base motion induces a rigid body displacement of the shell-disk system, such a rigid body motion gives rise to inertia forces both on the shell (axial u direction) and the disk; due to the particular configuration of the system (the disk mass is greatly larger than the shell mass) the inertia forces induced by the rigid motion of the shell are neglected, i.e. only the inertia forces of the disk are considered for which concern the rigid body motion. Moreover, in the following the attention will be focused on phenomena involving only axisymmetric or asymmetric shell like modes, i.e. beam like modes will be not considered because they are out of the excitation spectrum; this implies that rotations of the disk and displacements orthogonal to the shell axis can be neglected.

The disk axial displacement can be rewritten as:

$$S_{DISK}=u_B(t)+S_{Dx}(t) \tag{15}$$

where u_B and S_{Dx} are the base and the elastic displacements respectively.

The term S_{Dx} is already considered in the kinetic energy of the disk, in the present reduced problem it will be the only contribution to the disk kinetic energy.

The term u_B will be considered in evaluating the work of the inertia forces induced by the base motion (disk axial translation only): $\tilde{P}(t) = -m\ddot{u}_B(t)$; such load is considered uniformly distributed over the shell, the virtual work can be written accordingly:

$$W = \frac{\tilde{P}}{2\pi R}\int_0^{2\pi}\left[u(L,\theta,t) - \cancel{u(0,\theta,t)}\right]Rd\theta \tag{16}$$

where $u(L,\theta,t) = S_{Dx}$ and $u(0,\theta,t) = 0$ as the rigid body displacement is considered separately.

Using the modal expansion (13) the longitudinal displacement of the disk cannot be described with the natural coordinate S_{Dx} and the integral of eq. (16) must be evaluated in the modal basis.

Using Lagrange equations (13), a set of non-autonomous nonlinear ordinary differential equations is obtained; such system is then analyzed by using numerical time integration. The dissipation is added to the modal equation in order to use the modal damping ratio identified through experimental modal analysis, the resulting system is:

$$\ddot{z}_i(t) + 2\zeta_i\omega_i\dot{z}_i(t) + g_i(\mathbf{z}(t)) = Z_i(t) \tag{17}$$

where ζ_i is the modal damping ratio which must be set comparing the linear modes used in the expansion (13) with experimental modes, ω_i is the circular frequency of the mode corresponding to the i-th coordinate, g_i contains linear and nonlinear terms and Z_i is the external forcing projected on the modal basis.

5 LINEAR MODAL ANALYSIS

The system under investigation is described in Figures 2 and 3. A circular cylindrical shell, made of a polymeric material (P.E.T.) is clamped at the base by gluing its bottom to a rigid support (a disk that is rigidly bolted to a shaker, such disk is technically called “fixture”); the connection is on the lateral surface of the shell, in order to increase the gluing surface, see Figure 1. A similar connection is carried out on the top; in this case the shell is connected to a disk made of aluminium alloy, such a disk is not externally constrained; therefore, it induces a rigid body motion to the top shell end.

Table 1 shows theoretical and experimental natural frequencies concerning modes of interest for the present analysis: *k* means that the mode has *k*-1 nodal circumferences; *n* is the number of nodal diameters (beam modes can be considered *n*=1). In [4] a complete experimental, numerical and theoretical analysis is presented, the reader should read such paper for a full linear analysis of the problem under investigation. All modes are identified experimentally by using curve fitting techniques, present in LMS CADA-X, that give: frequency, modal damping ratio, and modal shape.

Mode		Experimental frequency [Hz]	*Theoretical frequencies* [Hz]
k	*n*		
1	0	314	322
1	6	791	802
1	7	816	797
1	5	890	927
1	8	950	888
1	9	1069	1046
1	4	1121	1191
1	10	1290	1251

Table 1. Experimental and theoretical natural frequencies.

In Figure 4 experimental mode shapes are reported, similar mode shapes obtained numerically are omitted for the sake of brevity [4].

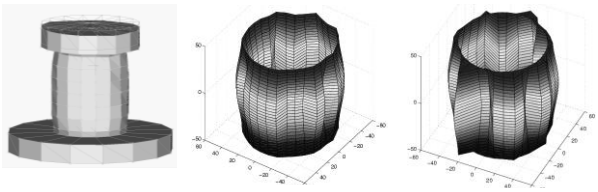

mode (1,0) (314Hz) mode (1,6) (791Hz) mode (1,7) (816Hz)

Figure 4. Mode shapes.

6 SEISMIC EXCITATION: NONLINEAR ANALYSIS

Such problem is investigated both theoretically and experimentally, the goal is a deep understanding of nonlinear phenomena appearing when the first axisymmetric mode is resonant: experiments evidenced that, when the shell is excited harmonically from the base with an excitation frequency close to the first axisymmetric mode, different dynamic scenarios appear and the energy pumped in the system at low frequency spreads over a wide range of the Fourier spectrum. The numerical analysis clarify the energy transfer mechanism and confirms the complexity of the scenario.

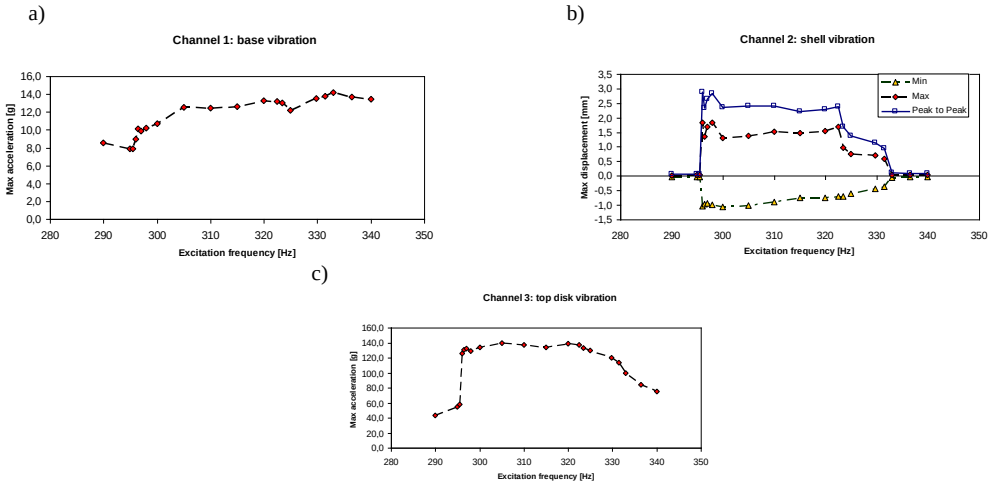

Figure 5. a) max amplitude of vibration (channel 1), b) max min and peak to peak of vibration (channel 2), c) max amplitude of vibration (channel 3)

6.1 *Experiments*

Tests are carried out using a seismic sine excitation, close to the resonance of the first axisymmetric mode (m=1, n=0).

The complexity and violence of vibrations due to nonlinear phenomena gave several problems to closed loop controllers of the shaking tables; therefore, an open loop approach was chosen, the excitation was set about 5-10 g.

Two accelerometers and a Laser telemeter are used to measure accelerations on base and top, and the displacement on the shell lateral surface: channel 1 records the base acceleration (the excitation) due to the shaking table; channel 2 records the displacement of the shell in radial direction, using a Micro Epsilon optoNCDT 2200 Laser Telemeter; channel 3 records the top disk acceleration.

a) b)

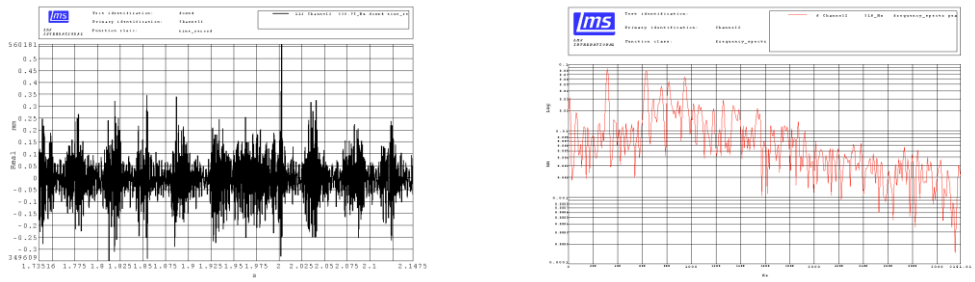

Figure 6. a) Time history from channel 2 (shell displacement); excitation freq 330.75 Hz. b) spectrum at 316Hz excitation.

Figures 5 a-c represent the amplitudes of vibration in terms of acceleration or displacement obtained when the excitation frequency is reduced. Channel 1 shows that the maximum excitation is between 8 and 14 g. The top disk vibration (channel 3) is magnified by the first axisymmetric mode resonance. However, close to 330 Hz, reducing the frequency, the linear resonance of the first axisymmetric mode is not present and the response is flat up to 295 Hz. In the same frequency range the shell experiences a violent vibration that appears suddenly, the amplitude passes from few microns to some millimetres; note that this corresponds to huge accelerations; for example if the amplitude is 3 mm, and we suppose it is purely harmonic (actually there are super-harmonic components) at 300 Hz, an approximate estimation of the acceleration is about 1100 g! In some previous experiments we measured up to 2000 g.

In Figure 6a one can observe that the response is not regular nor stationary; moreover, some spikes are visible. Figure 6b shows the spectrum of a nonstationary response, it shows that the energy spreads over a broadband frequency range.

Figure 7 clarifies that, when the nonlinear resonance takes place the response looses the periodicity, such analysis clearly shows that the phenomenon is extremely nonlinear.

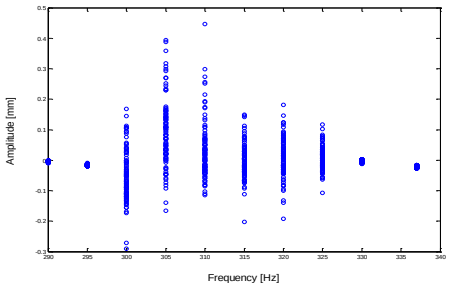

Figure 7. Bifurcation diagram of the Poincaré maps.

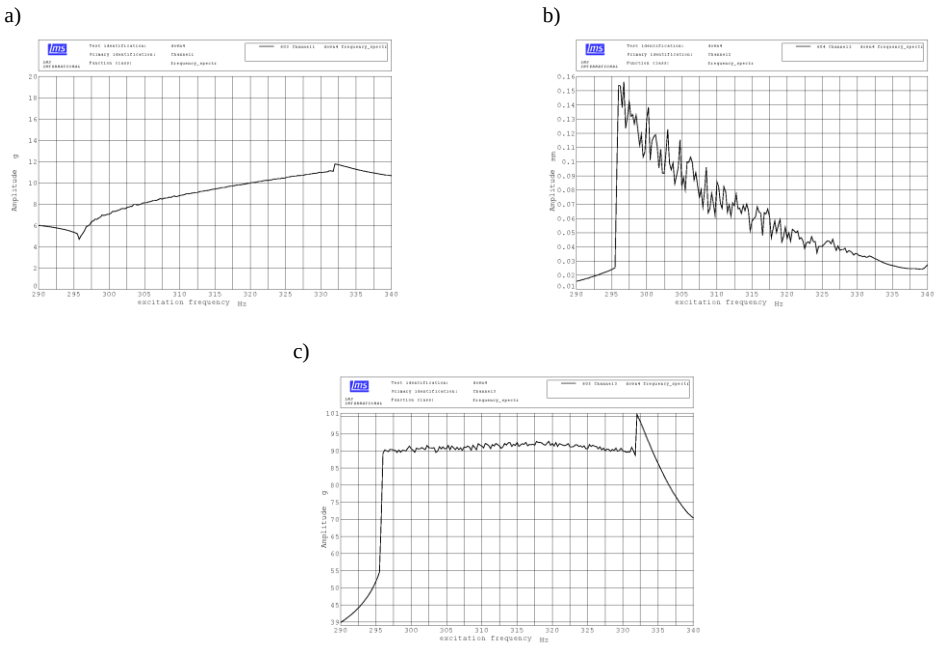

Figure 8. RMS of the response. a) base motion; b) shell vibration; c) top disk vibration.

The scenario represented in Figure 5 is referred to the maximum amplitude of vibration, which is not strictly related to the mechanical energy. In order to have an enhanced view on the phenomenon, useful for a physical interpretation, in Figure 8 the scenario is represented in terms of RMS. It is extremely interesting that, the RMS the top disk response is completely flat in a wide frequency range (Fig. 8 c), even though the excitation is not constant (Fig. 8 a), and the shell adsorbs a certain amount of energy (Fig. 8b).

The phenomenon disappears for low amplitudes of excitation, the threshold is currently under investigation.

Similar experiments were carried out by Mallon [6] who developed a model based on the Donnell's shallow shell theory: he found a saturation theoretically but experiments did not confirm his forecast. In [6] the shaker-shell interaction was modelled.

6.2 *Numerical analysis*

It is worthwhile to stress that the present analytical model has been developed in order to give a contribution toward the understanding of the previously mentioned phenomenon. In developing the model several data from experiments were extremely important to set up the numerical model; for example: Young modulus and density were separately measured by specific testing; modal damping was identified through experimental modal analysis including curve fitting of frequency response function (low amplitude linear dynamics); base excitation was measured during nonlinear dynamics experiments (see previous section).

Figure 9a shows the amplitude of oscillation (in terms of RMS) obtained numerically: a strong dynamic instability is observed in the frequency range (310-330Hz) that is narrower than the experimental one (295-330Hz); the agreement is qualitative in terms of amplitude. Figure 9b is useful for explaining the phenomenon, as single modal coordinate amplitudes are plotted; the

dynamic instability shows is complexity: several modes are activated with large amplitude. Figure 9c shows the spectrum of modal time histories at 322 Hz, the response seems chaotic.

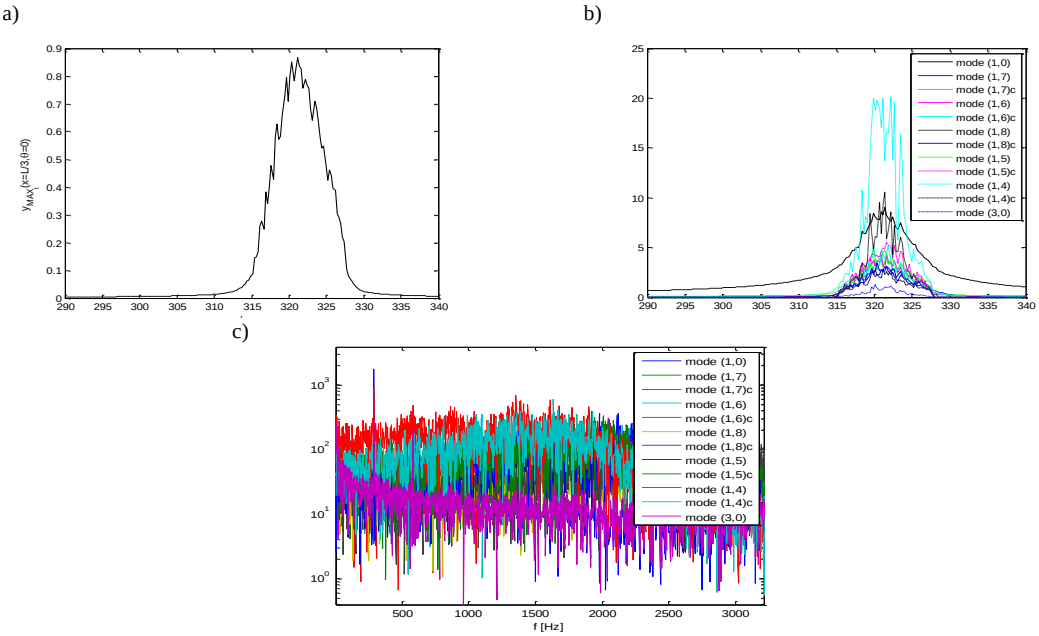

Figure 9. Numerical simulations. a) amplitude of oscillation on the shell; b) modal amplitudes; c) modal spectra at 322Hz excitation.

7 CONCLUSIONS

In this paper an experimental investigation on the nonlinear dynamics of circular cylindrical shells excited by a seismic excitation is presented. Experiments clearly show a strong nonlinear phenomenon appearing when the first axisymmetric mode is excited: the phenomenon leads to large amplitude of vibrations in a wide range of frequencies, it appears extremely dangerous as it can lead to the collapse of the shell; moreover, it appears suddenly both increasing and decreasing the excitation frequency and is extremely violent. By observing a strong transfer of energy from low to high frequency a conjecture can be made about the nonlinear interaction among axisymmetric (directly excited) and asymmetric modes. A saturation phenomenon regarding the vibration of the top disk is observed, this is associated with the violent shell vibration; the shell behaves like a energy sink, adsorbing part of the disk energy. The theoretical model partially confirms the conjecture.

References

1. A.W. Leissa, *Vibration of Shells*, NASA SP-288. Washington, DC: Government Printing Office. Now available from The Acoustical Society of America, 1993.

2. M. Amabili, M.P. Païdoussis, Review of studies on geometrically nonlinear vibrations and dynamics of circular cylindrical shells and panels, with and without fluid-structure interaction. *Applied Mechanics Reviews*, **56** (2003) 349-381.

3. V. A. Trotsenko and Yu. V. Trotsenko, Methods for calculation of free vibrations of a cylindrical shell with attached rigid body. *Nonlinear Oscillations*, **7**(2) (2004) 262-284.

4. F. Pellicano, "VIBRATIONS OF CIRCULAR CYLINDRICAL SHELLS: THEORY AND EXPERIMENTS", J. of Sound and Vibration, 2007, **303**, 154–170. doi:10.1016/j.jsv.2007.01.022.

5. N. Yamaki, *Elastic Stability of Circular Cylindrical Shells*, North-Holland, Amsterdam, 1984.

6. N. Mallon, *Dynamic Stability of thin-walled structures: A semi-analytical and experimental approach.* PHD thesis. Eindhoven Univ. of Technology Library, ISBN 978-90-386-1374-1.